13. Price, M. V., Waser, N. M., Irwin, R. E., Campbell, D. R. and Brody, A. K., Temporal and spatial variation in pollination of montane herb: a seven year study. *Ecology*, 2005, **86**, 2106–2116.
14. Brunet, J., Pollinators of the Rocky Mountine columbine: temporal variation, functional groups and associations with floral traits. *Ann. Bot.*, 2009, **105**, 1567–1578.
15. Shivanna, K. R., Kuriakose, G. and Sinu, P. A., Spatiotemporal variation in pollinators and their efficiency: a case study in cardamoms. In *Advances in Botany* (eds Vimla, Y., Trivedi, P. C. and Govil, C. M.), Indian Botanical Society Commemoration Volume, Pointer Publishers, Jodhpur, 2012, pp. 145–161.
16. de Nettancourt, D., *Incompatibility and Incongruity in Wild and Cultivated Plants*, Springer-Verlag, Berlin, 2001.
17. Sicard, A. *et al*., Genetics, evolution, and adaptive significance of the selfing syndrome in the genus *Capsella*. *Plant Cell*, 2011, **23**, 3156–3171.
18. Kalisz, S. and Vogler, D. W., Benefits of autonomous selfing under unpredictable pollinator environments. *Ecology*, 2003, **84**, 2928–2942.
19. Raju, A. J. S., Zafar, R. and Rao, S. P., Floral device for obligate selfing by remote insect activity and anemochory in *Wrightia tinctoria* (Roxb.) R.Br. (Apocynaceae). *Curr. Sci*., 2005, **88**, 1378–1380.
20. Dole, J. A., Reproductive assurance mechanisms in three taxa of the *Mimulus guttata* complex (Scrophulariaceae). *Am. J. Bot*., 1992, **79**, 650–659.
21. Wang, Y., Zhang, D., Renner, S. S. and Chen, Z., Self-pollination by sliding pollen in *Caulokaempferia coenobialis* (Zingiberaceae). *Int. J. Plant Sci*., 2005, **166**, 753–759.
22. Lekhak, M. M., Chavan, J. J., Janarthanan, M. K., Pai, I. K. and Yadav, S. R., Corolla elongation as an aid in self-pollination in *Rhamphicarpa longiflora* (Scrophulariaceae). *Curr. Sci*., 2011, **100**, 1624–1626.
23. Chen, L.-J. *et al.*, The anther steps onto the stigma for self-fertilization in a slipper orchid. *PLoS One*, 2012, **7**, e37478.
24. Eckert, C. G., Samis, K. E. and Dart, S., Reproductive assurance and the evolution of uniparental reproduction in flowering plants. In *Ecology and Evolution of Flower* (eds Harder, L. D. and Barrett, S. C. H.), Oxford University Press, New York, 2006, pp. 183–203.

ACKNOWLEDGEMENT. I thank the Indian National Science Academy (INSA), New Delhi for the award of INSA Honorary Scientist and Dr Rajesh Tandon for help in statistical analyses.

Received 12 September 2012; accepted 21 September 2012

Analysis of the potential of kimberlite rock spectra as spectral end member using samples from Narayanpet Kimberlite Field, Andhra Pradesh

Arindam Guha[1,*], D. Ananth Rao[1], S. Ravi[2], K. Vinod Kumar[1] and E. N. Dhananjaya Rao[3]

[1]Geosciences Division, National Remote Sensing Centre, Indian Space Research Organization, Balanagar, Hyderabad 500 037, India
[2]Geological Survey of India, Southern Region, Bandalguda, Hyderabad 500 068, India
[3]Department of Geology, Andhra University, Visakhapatnam 530 003, India

Mineral spectra as an end-member have been used for spatial mapping of the mineral deposits and associated potential lithovariants (altered rocks, etc.) while processing the remotely sensed hyperspectral data. But in nature, minerals occur in a mixture in rocks. Therefore, characterization of rock spectra is important. Here we study the role of texture, grain size and relative mineralogical abundances of constituent minerals in shaping the spectral features of the rock spectra in the visible–near infrared and shortwave infrared (VNIR–SWIR) domain. In this regard, analysis of kimberlite rock spectra is carried out to understand how absorption features of its constituent minerals are preserved in the spectral profiles of two different types of kimberlites with distinct mineral assemblages; one serpentine-rich and the other carbonate-rich. It has been observed that the spectral signature of the rock is controlled by the diagnostic absorption features of dominant constituent minerals. However, wavelength and depth of the diagnostic absorption feature of the dominant constituent mineral are modified in the rock spectra due to nonlinear spectral mixing with spectral features of other constituent minerals of the rock. It is observed that the spectral profiles of the rocks are not influenced by the fabric and grain size variation, except for the variation in the albedo or background reflectance of the spectral profiles. Spectral features of the rock also remain stable with the changes in the spectral measurement parameters. Therefore, it is concluded that the rock spectra can be used as an end-member or reference for spatial mapping of the economic rock instead of its constituent minerals.

Keywords: End-member, fabric, grain size, kimberlite, spectral features.

MAPPING of mineral deposits using 'spectral' features of minerals (significant to characterize the deposit) is well known. In this regard, airborne sensors such as Hymap,

*For correspondence. (e-mail: arindamisro@gmail.com)

AVIRIS, etc. were used for mapping of the economic mineral deposits (which are essentially rocks)[1–7]. The launch of Hyperion (space-borne hyper spectral imaging sensor with 10 nm spectral resolution operative within the spectral domain of 400–2500 nm) and ASTER (advanced space-borne thermal emission and reflection radiometer; a multi-spectral sensor with three spectral channels in the VNIR domain, six spectral channels in the SWIR domain and five channels in thermal infrared–TIR domain) in NASA's EO-1 platform have provided the desired data for upscaling the spectral signatures of minerals to these satellite data for spatial delineation of the economic mineral deposits[8–17]. Spectral signatures of minerals which have been used as the reference or end-member spectra for processing hyperspectral data either occur as an indicator or they themselves are the part of the mineral deposit. In all such cases, minerals are elementary constituents of the mineral deposits and therefore it is essential to understand how the spectral features of the constituent minerals behave in the composite rock. Collection and analysis of rock spectra is necessary in this regard. In the recent years, efforts have been made to develop spectral libraries of different minerals within the spectral domain of 350–14,000 nm that includes visible, near infrared, shortwave near infrared, and thermal wavelengths[18–20]. Moreover, spectral libraries of rocks are also available in the thermal region of the electromagnetic domain (broadly within the spectral range of 2–14 μm or 2,000 to 14,000 nm). But visible–near infrared and shortwave infrared (VNIR–SWIR) electromagnetic domains are not optimally used for rock spectroscopy. However, in the recent past, spectral libraries for few rocks have been developed within this spectral domain also. Moreover, spectral library for rocks of the Indian geological province is not available till date. Records of the comparative analysis of a spectral features of a rock with the spectral features of its constituent minerals are also not available. This information is essential to understand whether the spectral feature of the constituent mineral is sufficient to characterize the rock in terms of spectral behaviour of the rock, or whether we require the rock spectra. It is also important to understand whether the spectral parameters of the rock spectra are stable with the variation in grain size, fabric of the rock and also with the change in the measurement set-up for spectral data collection. This understanding would be necessary for qualifying a rock spectrum as an end-member or standard reference. Characterization of rock spectrum requires analysis of each absorption feature in it in the light of the spectral features of the constituent minerals, which can be identified based on X-ray diffraction (XRD) analysis. Once this is done, it would isolate one or two absorption features as the diagnostic spectral feature of the rock. Further, it is essential to understand how grain size, texture (mutual juxtaposition of the minerals) and mineralogy affect in shaping the spectral features of the rock.

In the present study, this has been achieved by integrated analysis of the rock spectra of kimberlite in the light of the parameters like texture, grain size and mineralogy. Effect of variations in the ground sampling diameter and phase angle on shaping the spectral profiles during collection of spectral data has also been studied.

Kimberlite is known for hosting diamond and also has its own petrogenetic importance. Satellite-based studies used spectral feature of 'serpentine' as a criterion for spatial mapping of kimberlite[21]. However, the roles of texture, grain size and optical coupling of different spectral features of the associated minerals in influencing the spectral features of serpentine were not examined in earlier studies. Therefore, spectral profiles of different types of kimberlite are studied to understand whether mineralogy alone contributes to the spectral feature of kimberlite or texture and grain size also have an influence in governing the spectral profiles. The study would help to understand whether rock spectra can be regarded as an end-member for spectral mapping of the target.

The study area is situated near Narayanpet in Andhra Pradesh, India. The area is well known for the occurrences of kimberlite. Geologically, the kimberlites of Narayanpet Kimberlite Field (NKF) are located in the Eastern Dharwar Craton (EDC) of South India. The NKF is situated at western part of Mahabubnagar district, Andhra Pradesh and eastern part of the adjoining Gulbarga district, Karnataka. The characteristic mineral assemblages and textures of the kimberlite bodies indicate that these correspond to hypabassal or root-zone kimberlites[22,23]. These pipes, in general, occur as very small bodies, about a few square metres in size. NKF kimberlite

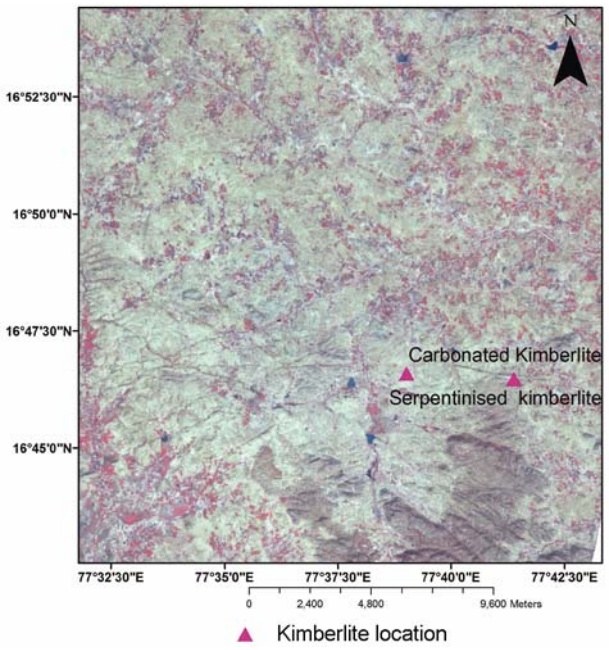

Figure 1. Location of serpentinized kimberlite and carbonate-rich kimberlite shown in the false colour composite (FCC) of ASTER image (R, third band; G, Second band; B, First band).

pipes have not yet been proved to be diamondiferous. Field locations of the kimberlite pipes studied in this work are plotted on false colour composite (FCC) satellite image from ASTER data (Figure 1). Kimberlites studied here are dominantly made up of minerals which have diagnostic spectral signatures in the VNIR–SWIR domain. These minerals belong to the serpentine and carbonate group. They occur as psedumorphs after primary minerals and also as monomineralic hydrothermal segregations. Many researchers are of the opinion that external silica-rich fluid invading kimberlites just after their emplacement, are responsible for the formation of the serpentine group of minerals in the kimberlites. Experimental data show that the presence of external fluid is responsible for increasing the serpentine content from 25% by volume to 75% by volume, which can further increase to 80% if the external fluid contains silica[24,25]. Carbonate minerals (calcite or dolomite) in kimberlite are either primary (occur as primary ground mass) or secondary (occur as replacement mineral) in origin. Kimberlites from Narayanpet area studied here consist of carbonate and serpentine group of minerals approximately 80% by volume of the rock. One group is distinctly carbonate-rich and the other serpentine-rich.

In the present study rock spectra of two different types of kimberlites are analysed in the light of spectral features of dominant or spectrally conspicuous mineral spectra. Relative abundance of mineral phases of each type of kimberlite is determined using XRD. The methodology is subdivided into five broad parts: sample preparation, spectral data collection, spectral data processing, mineralogical analysis of spectral data and analysis of rock spectra in the light of the variations in the rock fabric and measurement set-up.

In this regard, three to four large samples from each type of kimberlite are collected. From each sample three sub-samples are prepared, one each for spectral profile collection, XRD and for pulverization.

Rock samples cut into rectangular chips of $3'' \times 3''$ to $5'' \times 7''$ are used for spectral profile collection. The specified size of the samples used for spectroscopic study is well within the norms of the sample size specification of the Jet Propulsion Laboratory (JPL), NASA, USA[26]. In fact, the size is larger than the samples used in JPL. This larger size of the sample is essential to record the textural variability for understanding its role in spectroscopy of the rock and it is also suitable for reducing the contribution from the adjacent source(s) in the measured radiance in the laboratory. Another set of kimberlite samples was pulverized and sieved into different size ranges (60–100 μm and less than 100 μm) to understand how a homogeneous mixture of rock powder of specified grain size range spectrally behaves in comparison to the spectral profile of the consolidated rock.

Laboratory measurement of spectral signature is the basis for understanding the spectral response of different kimberlite rock samples in controlled environment. The spectroradiometer used had good signal-to-noise ratio with fine spectral resolution (3 nm @ 350–1,050 nm and 10 nm @ 1,000–2,500 nm)[27] and finer spectral sampling interval (1.4 nm @ 350–1,050 nm and 2 nm @ 1,000–2,500 nm). The sampling interval of the spectroradiometer was finer than the spectral resolution of the sensor to reduce the system noise while measuring the finer spectral feature. The system noise has been calibrated by the manufacturer and it is wavelength-dependent (noise equivalent δ radiance: VNIR 1.1×10^{-9} W/cm^2/nm/sr @ 700 nm; NIR 2.8×10^{-9} W/cm^2/nm/sr @ 1,400 nm; NIR 5.6×10^{-9} W/cm^2/nm/sr @ 2,100 nm)[28]. The reflectance of the rock surface was measured based on the ratio of the radiant flux actually reflected by a sample surface to the radiant flux reflected by an ideal lossless and perfectly diffused standard optical surface irradiated in exactly the same way as the sample[29]. The reference surface which is a perfectly lossless and ideal diffuse surface, is known as a reference panel in the field of reflectance spectroscopy. Despite considerable developments in the field of spectroscopy, reference panels used for the purpose of spectral profile collection are neither perfectly reflecting nor perfectly diffuse, because both these properties are wavelength-dependent[30]. In order to take care of the above issue, Spectralon is used as a calibration panel in the present study. It has a high and stable reflectance throughout the optical region. Moreover, the panel is easily washable and therefore can be properly maintained despite its tendency in generating a static charge due to insects and dust particles clinging to it under some conditions. Procedures for calibration of reference panels are also well discussed in the spectroscopic literature[31].

Sample reflectance is measured by pointing 'vertically' the measurement gun which contains the fibre optics of the sensor (Figure 2). The light source is used to illuminate the sample at about 45° angle (with respect to the

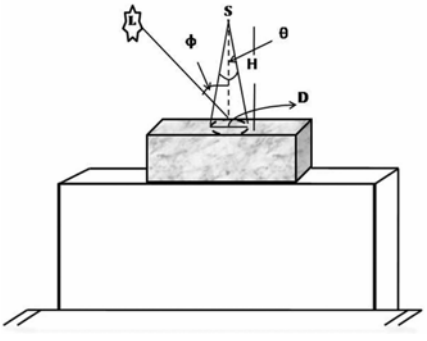

Figure 2. Schematic diagram showing the measurement set-up for collecting spectral profiles of different rocks. Here L is the light source, S the position of the optics of the spectroradiometer, θ the field of view of optics of the spectroradiometer, ϕ the phase angle of measurement, H the distance of the optics of the spectroradiometer from the surface of the sample, and d is the diameter of the area over the sample surface for which the spectral profiles are collected. Sample is shown schematically as a rectangular block.

imaginary vertical line drawn over the sample) and the measurement is taken by keeping the fore optics of the spectroradiometer vertically over the sample with the phase angle (ϕ) about 45° (phase angle is the angle between the illumination source and measurement point) to reduce the specular component of reflected energy in the measured signal (Figure 2). The reflected energy resulted by volume scattering of the rock is a true representative of the internal chemistry, as the volume scattering process allows incident radiation to get reflected from the multiple grain boundaries of different constituent minerals. On the other hand, specular component of reflected energy is the result of the surface roughness and is restricted to a few mineral grain boundaries. For the purpose of spectral profile collection, field of view is 25°. The measurement gun is adjusted vertically in such a position so that it can create a ground sampling diameter (GSD) D to cover all the variability in the sample (Figure 2). The diameter of the sample spot exposed for spectral profile generation can be estimated from the following mathematical relation:

$$D = H \times 2 \times \tan\theta/2,$$

where D is the diameter of the measurement zone or GSD of spectral measurement, H the height of the measurement and θ is the field of view. One can move up or down the measurement gun to collect the required representative area of the rock. For collecting the spectral profiles, 20 observations per sample spot are recorded. Four sample spots in each rock sample are studied to understand the variability of the spectral profile across the sample (Figure 3). The mean spectral profile of each type of the kimberlite is derived by averaging the characteristic spectral profile of each spot. Spectral profiles of carbonate-rich kimberlite and serpentine-rich kimberlite are also measured by changing GSD and also by changing the angle between the light source and fore optics of the spectroradiometer (Figure 4).

Spectral signatures of kimberlite samples thus collected are processed using standard software (the software are an integral part of Fieldspec 3 Spectroradiometer manufactured by Analytical Spectral Device Inc.) to remove the insignificant kinks and to derive the spectral profiles with the characteristic 'spectral features'. In order to remove the infinitely small kinks, 50 scans for each sample spot are taken and then averaged before providing the individual spectral measurements of the rock samples. Smaller kinks are often the result of noise in the system. Absorption signatures of kimberlite rock samples are studied based on waveform characterization. Here, the spectral profiles are normalized for spectrometric analysis to derive wavelength, depth, width, asymmetry, area, etc. of the absorption feature[32]. These are known as spectrometric parameters. In this respect, the upper convex hull of a spectral profile (imaginary line joining the highest reflectance values of the spectral curve or joining the inflection points indicating baseline reflectance on the either side of a absorption feature) is derived and used as an enveloping line touching the spectral curve at the point of highest reflectance value on the target spectra having no absorption features. This imaginary line is also known as a continuum. Next, the original reflectance curve is normalized with respect to the continuum to derive width, depth and asymmetry of each characteristic absorption feature[33]. These spectrometric parameters of absorption features of a spectra are also shown schematically in Figure 5. Each absorption feature has certain spectrometric parameters. Amongst these, absorption band position is a crucial parameter, which is regarded important in recognizing the mineral, as the wavelength at which absorption takes place

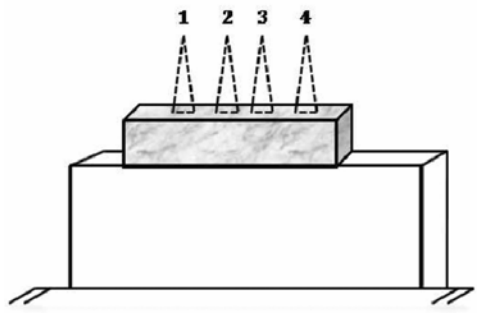

Figure 3. Schematic diagram of measurement set-up showing how spectral profiles are collected from different spots over the same sample surface. Sample is shown schematically as a rectangular block.

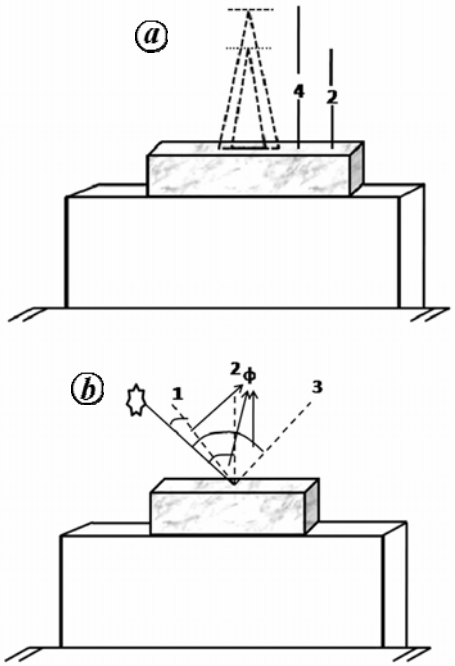

Figure 4. ***a***, Schematic diagram showing how the distance of measurement optics is lowered from 4 to 2 cm to collect the spectral profiles for sample areas of different size (diameter). ***b***, 1, 2 and 3 are the relative positions of the optics of the spectroradiometer with respect to the light source (demarcated as star) for collecting the spectral profile of a rock sample with phase angle 0°, 45° and 90°.

is related to the atomic process resulting from the interaction of electromagnetic energy with the atomic framework of the mineral. The absorption band position (λ) is defined as the band having the minimum reflectance value over the wavelength range of the absorption feature. The relative depth, d, of the absorption feature can be derived from the reflectance value at the shoulders minus the reflectance value of the absorption band minimum (Figure 5). In addition, the width of the absorption feature, W, is another important spectrometric property. Width of absorption signature signifies the amount of energy absorbed and width of the electromagnetic domain across which the absorption takes place. W is given by

$$W = A_{\text{all}}/2d,$$

where A_{all} is the sum of the total area. The symmetry factor S of the absorption feature is defined as

$$S = 2(A_{\text{left}}/A_{\text{all}}) - 1.$$

where A_{left} is the area at the left, and A_{right} the area on the right of the absorption band minimum under the convex hull enclosing the absorption feature (Figure 4). The asymmetry or symmetry factor of the spectral feature ranges from –1.0 to 1.0, in which S would be 0 for a symmetric absorption feature.

Each rock spectrum has a few characteristic spectral features or absorption features. These features are a result of the spectral signature of the dominant constituent mineral(s). The relative abundance of the mineral in each rock sample is derived from XRD analysis (Table 1). The spectral signature of the dominant mineral of each rock type is compared with the respective rock spectrum to identify the diagnostic spectral feature of the rock with reference to the diagnostic spectral features of the constituent minerals.

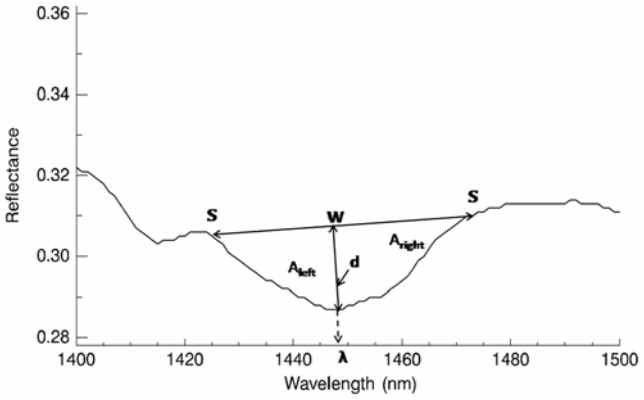

Figure 5. Schematic diagram showing different spectrometric parameters of a spectral feature. λ is the wavelength of the absorption feature, w the width of the absorption feature, S the shoulder of the absorption feature, and A_{left} and A_{right} are the areas to the left and right of the maximum depth of the spectral feature generally used for calculating the symmetry factor or asymmetry.

Rock spectra are compared with the spectral profiles of the pulverized rock samples with different grain size ranges to understand the role of the fabric of the consolidated rock in modifying the spectral features in the reflectance profile of the rock. Intra-rock spectral variations are also studied by taking the multi-spot spectral measurements. In addition, how phase angle and GSD of spectral measurements govern the spectral profiles of the rock are also studied.

The spectral feature of a mineral is of paramount interest and spectral signature or absorption feature of the reflectance profile of the mineral is often used for its diagnosis. Spectral libraries have been developed for different minerals (e.g. USGS spectral library of minerals developed by JPL). These spectral libraries are used to analyse the spectral feature of a rock. It is also well understood that the wavelength of absorption of the diagnostic spectral feature of each type of kimberlite is governed by the spectral feature of the dominant constituent mineral. However, in many cases, the wavelength of absorption of the diagnostic feature of the rock is displaced with respect to the spectral feature of the constituent minerals along the wavelength axis[28]. In the present study, an attempt is made to understand the spectral profiles of serpentinized and carbonate-rich kimberlites with reference to mineralogy, texture and grain size. In addition, efforts are also made to understand how spectral profiles are influenced by GSD of measurement and also by the angle of measurement with reference to the illuminator.

The spectral profiles of serpentinized kimberlite and carbonate-rich kimberlite were analysed with reference to the spectral profiles of the dominant constituent mineral. The relative dominance of the constituent mineral is ascertained by XRD data for the samples (Table 1).

Serpentine has a diagnostic spectral feature at 2,326 nm, whereas calcite has a diagnostic absorption feature within the spectral domain of 2,330–2,335 nm (refs 34 and 35).

Table 1. X-ray diffraction data of serpentinized and carbonate-rich kimberlite pipes showing the relative abundance of the constituent minerals[28]

Kimberlite type	Minerals	Relative abundance detail
Serpentinized kimberlite	Lizardite	Major
	Phlogopite	Small amount
	Frosterite	Traces
	Perovskite	Traces
	Andradite	Good amount
	U\Spinel	Traces
Carbonate-rich kimberlite	Calcite	Major
	Dolomite	Small amount
	Perovskite	Small amount
	Andradite	Small amount
	*Smectite	Traces

*Indicate that the confirmation is further required with other set of data.

It has been observed that the spectral profiles of the serpentinized and carbonate-rich kimberlites are governed by the spectral profiles of the dominant mineral; however, the wavelength of absorption of the diagnostic spectral feature of the dominant constituent minerals, i.e. lizardite for serpentinized kimberlite and calcite for carbonate-rich minerals are shifted (20 nm for serpentinized kimberlite and 30 nm for carbonate-rich kimberlite) towards the lower wavelength (Figure 6)[28]. This can be attributed to the optical coupling of different spectral features of the associated minerals. Moreover, the width and depth of the diagnostic spectral feature of serpentine and carbonate minerals are subdued in the serpentine-rich and carbonate-rich kimberlites (Figure 6). The variabilities of width and depth have implication on using the spectral feature for target detection. The larger the depth and width of the spectral feature, better would be its detection based on spectral feature. As spectral features of rocks are subdued in terms of depth and width (as it is observed here), it would be difficult to delineate the mixed target like rock as compared to that from the corresponding constituent mineral based on absorption spectroscopy.

Role of grain size in shaping the spectral curve of minerals is well understood[36]. It is known that the spectral absorption features remain subdued (i.e. with lesser absorption depth) in fine-grained minerals in comparison to coarse-grained minerals. It is also understood that the finer grain size mineral has higher absolute reflectance in comparison to coarser grain size mineral due to higher surface area offered by the fine particles. But how spectral profiles of the consolidated rock vary in comparison to the different size fractions of rock powder has not been studied earlier, although efforts were made to characterize mineral-mixture based on the grain size variability[36]. In the present study an attempt is made to record such variability. In this regard, the rock samples, one each for serpentinized kimberlite and carbonate-rich kimberlite and their respective pulverized size fractions are analysed. Rock powders of two size ranges are prepared. The coarser variety has size range from 60 to 100 mesh (250–149 μm); whereas the finer variety has grain size finer than 100 mesh (less than 149 μm). It is observed that the finer-grained homogenous powder of kimberlite has higher reflectance values in comparison to the coarser grain size fraction and consolidated serpentinized kimberlite (Figure 7 *a*). On the other hand, powdered rock of carbonate-rich kimberlite (of both grain sizes) has higher reflectance compared to the consolidated rock (Figure 7 *b*).

The major observation from the comparison of the powdered rock sample with the consolidated rock is that the consolidated rock has lower background reflectance than the corresponding rock powder, although the relative position of the wavelength of absorption of the spectral features of the powdered sample and the consolidated rock is the similar (Table 2). Therefore, the fabric of the

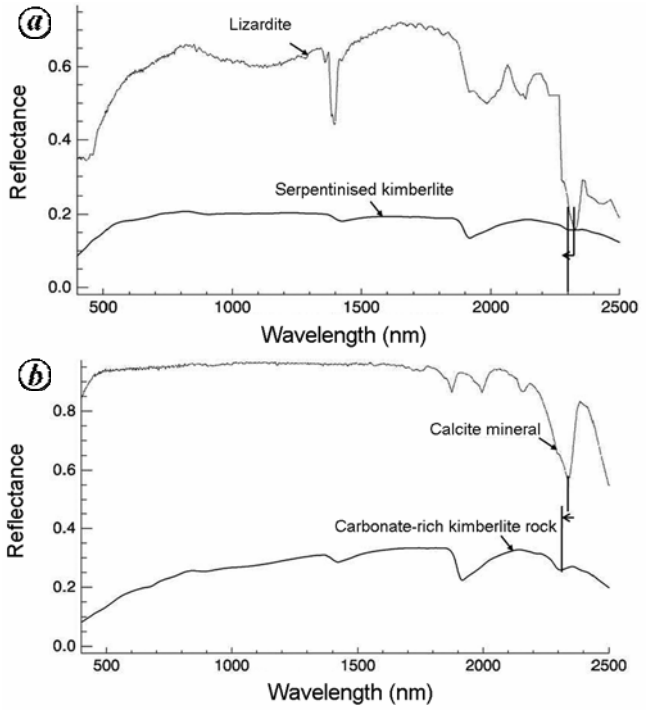

Figure 6. ***a***, Spectral profile of serpentinized kimberlite plotted with that of the lizardite mineral (the most abundant mineral in the rock sample); ***b***, Spectral profile of carbonate-rich kimberlite plotted with that of the calcite mineral (the most abundant mineral in the rock sample). See Table 1.

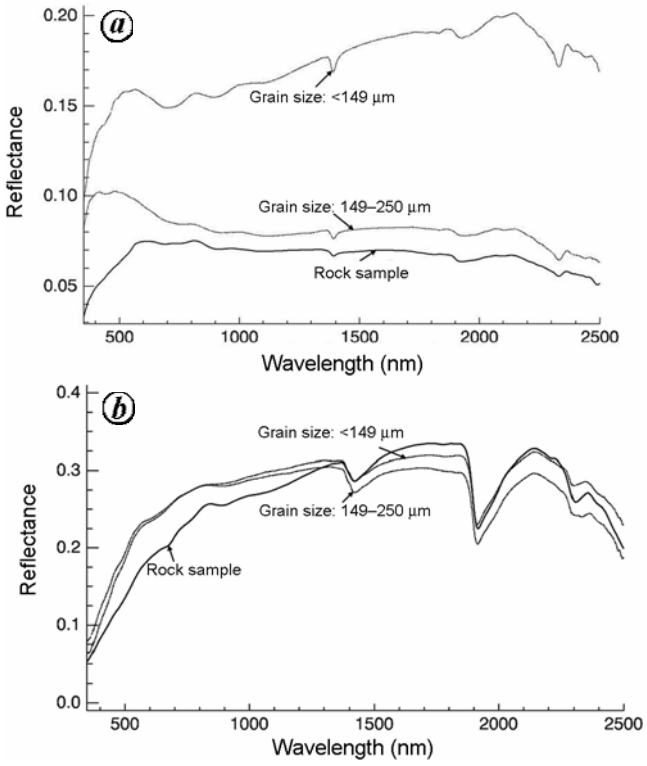

Figure 7. Spectral profile of serpentinized kimberlite (***a***) and carbonate-rich kimberlite (***b***) plotted with those of the powdered samples of different grain sizes (size range).

Table 2. Spectrometric properties of serpentinized and carbonate-rich kimberlite

Samples						
Kimberlite type	Sample type	Wavelength (nm)	Depth	Width	Area	Asymmetry
Serpentinized kimberlite						
	Rock sample	2325	0.0784	71	10.527	–0.003
	Kimberlite powdered sample (60–100 mesh size)	2326	0.117	70	12.959	0.021
	Kimberlite powdered sample (<100 mesh size)	2325	0.074	63	4.495	–0.352
Carbonate-rich kimberlite						
	Rock sample	2301	0.104	54	5.795	–0.113
	Kimberlite powdered sample (60–100 mesh size)	2299	0.074	63	4.495	–0.352
	Kimberlite powdered sample carbonated kimberlite (<100 mesh size)	2299	0.050	44	2.253	–0.180

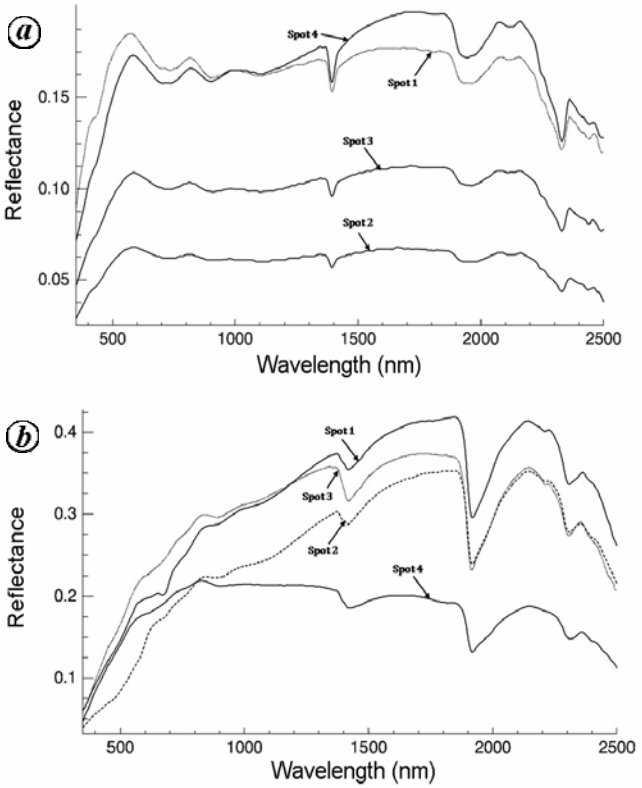

Figure 8. ***a***, Spectral profiles of different parts/spots of (***a***) serpentinized kimberlite and (***b***) carbonate-rich kimberlite.

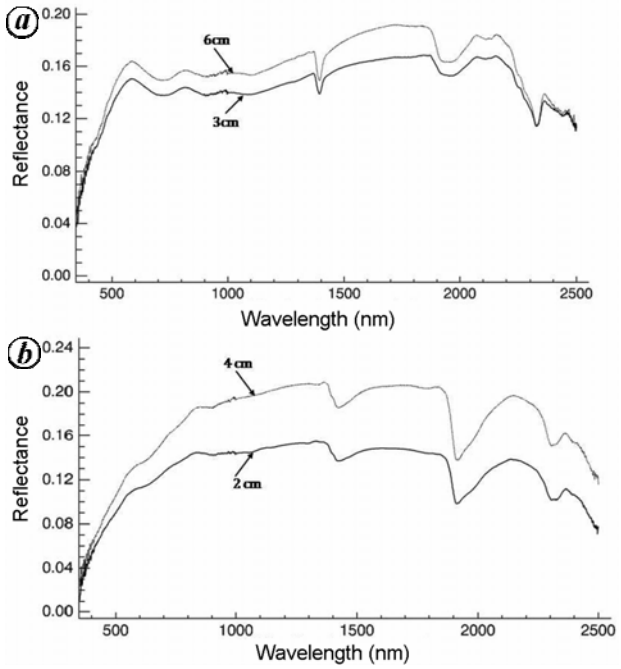

Figure 9. ***a***, Spectral profiles of serpentinized kimberlite measured using optics of the spectrodiometer with different heights from the top of the surface of the rock sample. ***b***, Spectral profiles of carbonate-rich kimberlite collected from different heights.

consolidated rock does not affect the wavelength of absorption of the spectral features, which is the key to deciphering the rock based on the spectral signature.

In addition, four sample spots of each type of kimberlite are studied by moving the relative position of the foreoptics of the spectroradiometer with respect to sample surface to record the intra-sample variability of the spectral feature. The measurement set-up for collecting the spectral profiles for the multiple spots of the sample is illustrated in Figure 3, where the height of the spectral measure remains the same, but the relative position of the spectroradiometer is shifted laterally to cover the adjacent part of the sample. It has been observed that the spectral profiles of the rock remain the same for each and every spot for serpentinized and carbonate-rich kimberlite (Figure 8). Specially, the wavelength of absorption of the spectral feature is found to be consistent for all the spots. It is also observed that smaller spot size of a few centimetres is sufficient to record the mineralogical and textural artefacts of the fine-grained rock sample like kimberlite and therefore changing the size of the spots (this is achieved by moving the measurement optics up and down with respect to sample surface) within the rock sample

would not alter the spectral characteristic of the rock (Figure 9).

The spectral properties of the natural surface are essentially directional, i.e. the amount of reflectance energy received from a natural surface is governed by the angle between the illuminator and the reflectance measurement optics. This angle is known as the phase angle. The height of the measurement optics with respect to the sample surface is another criterion which influences the spectral profiles of a sample. For recording the spectral profiles of the rock with respect to different phase angles, the measurement optics was kept near parallel, at 45° and perpendicular to the light source, which is essentially a well-calibrated argon lamp (Figure 4 *b*). Relative height of the sensor optics with respect to the sample surface was changed from 2 to 4 cm to record the variability of the spectral profiles of the rock due to the varying spot size resulting from the variable height of the measurement optics with reference to the surface of the sample (Figure 4 *a*). It has been observed that the change in phase angle does not affect the position of the wavelength of the spectral features of the rock; however, background reflectance of the spectral profiles would vary for each phase angle of measurement (Figure 10). Similarly, change in the height of spectral data collection only changes the area for which spectral profile is collected; it does not contribute to change in the wavelength of the spectral feature of the rock spectra. However, the background reflectances of the spectral profiles are modified (Figure 9).

Although spectral signatures of the rocks (in the present case serpentinized and carbonate-rich kimberlites) are shaped by the spectral feature of the dominant constituent mineral(s), the wavelength of absorption, width and depth of absorption of diagnostic spectral features are modified in the rock spectra in comparison with the respective diagnostic spectral features of the constituent mineral(s). Therefore, it can be concluded that it is better to use the spectral feature of the rock than the spectral feature of the constituent mineral for spectral mapping. Therefore, the rock spectra may be regarded as the elementary input or end-member for the purpose of spatial mapping of rock formation. The end-member or elementary input must be consistent and wavelength of the spectral feature of the rock should not be perturbed by geometry of measurement and textural variability. In the present work, it was observed that the wavelength of absorption of spectral features of a rock did not vary or shift with the change in the phase angle and the distance between the measuring optics and the surface of the sample. Also, spectral features of the consolidated rock did not change with the change in grain size. Except for the variation in the background reflectance value; wavelength of absorption of spectral features, remained insensitive to intra-sample textural variability.

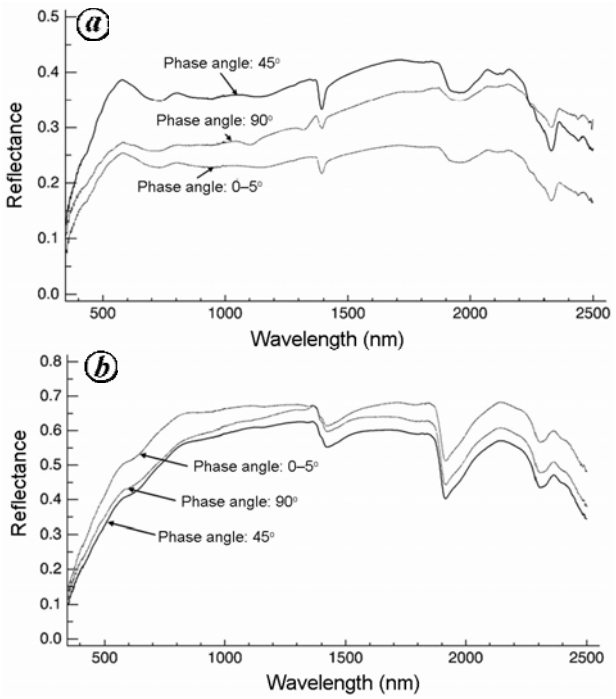

Figure 10. Spectral profiles of serpentinized kimberlite (***a***) and carbonate-rich kimberlite (***b***) measured with different phase angles.

1. Bedini, E., Remote sensing of environment mapping lithology of the Sarfartoq carbonatite complex, southern West Greenland, using HyMap imaging spectrometer data. *Remote Sensing Environ.*, 2009, **113**, 1208–1219.
2. Bedini, E., Mineral mapping in the Kap Simpson complex, central East Greenland, using HyMap and ASTER remote sensing data. *Adv. Space Res.*, 2011, **47**, 60–73.
3. Boardman, J. W. and Kruse, F. A., Automated spectral analysis: a geological example using AVIRIS data, north Grapevine Mountains, Nevada. In Thematic Conference on Geological Remote Sensing, TX, ERIM (ed.) San Antonio, 1994, pp. 407–418.
4. Galvao, L., Relationships between the mineralogical and chemical composition of tropical soils and topography from hyperspectral remote sensing data. *ISPRS J. Photogramm. Remote Sensing*, 2008, **63**, 259–271.
5. Green, R. O. *et al.*, Imaging spectroscopy and the airborne visible/infrared imaging spectrometer (AVIRIS). *Remote Sensing Environ.*, 1998, **65**, 227–248.
6. Kruse, F. A., Mineral mapping with AVIRIS and EO-1 Hyperion. Jet Propulsion Laboratory Publication 04-6 (CD-ROM), 2003, pp. 149–156.
7. Kruse, F. A. and Perry, S. L., Improving multispectral mapping by spectral modeling with hyperspectral signatures. *J. Appl. Remote Sensing*, 2009, **3**, 033504.
8. Aboelkhair, H., Ninomiya, Y., Watanabe, Y. and Sato, I., Processing and interpretation of ASTER TIR data for mapping of rare-metal-enriched albite granitoids in the Central Eastern Desert of Egypt. *J. Afr. Earth Sci.*, 2011, **58**, 141–151.
9. Azizi, H., Tarverdi, M. A. and Akbarpour, A., Extraction of hydrothermal alterations from ASTER SWIR data from east Zanjan, northern Iran. *Adv. Space Res.*, 2010, **46**, 99–109.
10. Di Tommaso, I. S. and Rubinstein, N., Hydrothermal alteration mapping using ASTER data in the Infiernillo porphyry deposit, Argentina. *Ore Geol. Rev.*, 2007, **32**, 275–290.
11. Gad, S. and Kusky, T., ASTER spectral ratioing for lithological mapping in the Arabian–Nubian shield, the Neoproterozoic Wadi Kid area, Sinai, Egypt. *Gondwana Res.*, 2007, **11**, 326–335.

12. Moghtaderi, A., Moore, F. and Mohammadzadeh, A., The application of advanced space-borne thermal emission and reflection (ASTER) radiometer data in the detection of alteration in the Chadormalu paleocrater, Bafq region, Central Iran. *J. Asian Earth Sci.*, 2007, **30**, 238–252.
13. Pour, A. B. and Hashim, M., The application of ASTER remote sensing data to porphyry copper and epithermal gold deposits. *Ore Geol. Rev.*, 2012, **44**, 1–9.
14. Rajendran, S., Al-Khirbash, S., Pracejus, B., Nasir, S., Al-Abri, A. H., Kusky, T. M. and Ghulam, A., ASTER detection of chromite bearing mineralized zones in Semail Ophiolite Massifs of the northern Oman Mountains: exploration strategy. *Ore Geol. Rev.*, 2012, **44**, 121–135.
15. Rowan, L. C., Mars, J. C. and Simpson, C. J., Lithologic mapping of the Mordor, NT, Australia ultramafic complex by using the Advanced Spaceborne Thermal Emission and Reflection Radiometer (ASTER). *Remote Sensing Environ.*, 2005, **99**, 105–126.
16. Rowan, L. C., Schmidt, R. G. and Mars, J. C., Distribution of hydrothermally altered rocks in the Reko Diq, Pakistan mineralized area based on spectral analysis of ASTER data. *Remote Sensing Environ.*, 2006, **104**, 74–87.
17. Zhang, X., Pazner, M. and Duke, N., Lithologic and mineral information extraction for gold exploration using ASTER data in the south Chocolate Mountains (California). *ISPRS J. Photogram. Remote Sensing*, 2007, **62**, 271–282.
18. Cloutis, E. *et al.*, Detection and discrimination of sulfate minerals using reflectance spectroscopy. *Icarus*, 2006, **184**, 121–157.
19. Cloutis, E. A., Hyperspectral geological remote sensing: evaluation of analytical techniques. *Int. J. Remote Sensing*, 1996, **17**, 2215–2242.
20. Cloutis, E. A. *et al.*, The 506 nm absorption feature in pyroxene spectra: nature and implications for spectroscopy-based studies of pyroxene-bearing targets. *Icarus*, 2010, **207**, 295–313.
21. Kruse, F. A. and Boardman, J. W., Characterization and mapping of kimberlites and related diatremes using hyperspectral remote sensing. IEEE Aerospace Conference Proceedings, Big Sky, MT, 2000, pp. 299–304.
22. Haggerty, S. E. and Birkett, T., Geological setting and chemistry of kimberlite clan rocks in the Dharwar Craton, India. *Lithos*, 2004, **76**, 535–549.
23. Murthy, D. S. N. and Dayal, A. M., Geochemical characteristics of kimberlite rock of the Anantapur and Mahbubnagar districts, Andhra Pradesh, South India. *J. Asian Earth Sci.*, 2001, **19**, 311–319.
24. Podvysotskiy, V. T., Serpentine and carbonate mineralisation in the kimberlites. *Int. Geol. Rev.*, 1985, **27**, 810–823.
25. Schumacher, J. C., Serpentine in kimberlite: an indicator of water-rich primary or externally-derived fluid? In European Mineralogical Conference, 2012, vol. 1, p. 593.
26. Baldridge, A. M., Hook, S. J., Grove, C. I. and Rivera, G., The ASTER spectral library version 2.0. *Remote Sensing Environ.*, 2009, **113**, 711–715.
27. ASD Inc, 2012. Field spec specification; http://www.asdi.com/products/fieldspecspectroradiometers/fieldspec-3-portable-spectro-radiometer
28. Guha, A., Ravi, S., Vinod Kumar, K. and Dhananjaya Rao, E. N., Reflectance spectroscopy of kimberlites and its scope in exploration – a case study in the Narayanpet kimberlite-field, Andhra Pradesh, India. *J. Earth Syst. Sci.*, 2012 (in press).
29. Nicodemus, F. F., Richmond, J. C., Hsia, J. J., Ginsberg, I. W. and Limperis, T. L., Geometrical considerations and nomenclature for reflectance. National Bureau of Standards Monograph, Washington, 1977, p. 20402.
30. Bruegge, C. J., Chrien, N. and Haner, D., A Spectralon BRF database for MISR calibration applications. *Remote Sensing Environ.*, 2001, **76**, 354–366.
31. Biggar, S. F., Labed, J., Santer, R. P. and Slater, P. N., Laboratory calibration of field reflectance panels. In Proceedings of SPIE – The International Society for Optical Engineering (ed. Slater, P. N.), Orlando, Florida, 1988, pp. 232–240.
32. Okada, K. and Iwashita, A., Hyper-multispectral image analysis based on waveform characteristics of spectral curve. *Adv. Space Res.*, 1992, **12**, 433–442.
33. Van Der Meer, F. D., De Jong, S. M. and Bekker, W. H., Imaging spectrometry: basic analytical techniques. In *Imaging Spectrometry: Basic Principles and Prospective Applications* (eds Van der meer, F. D. and De Jong, S. M.), Springer, 2001, pp. 15–61.
34. Trude, King, V. V. and Clark, R. N., Spectral characteristics of chlorites and Mg-serpentines using high-resolution reflectance spectroscopy. *J. Geophys. Res.*, 1989, **94**, 13997–14008.
35. Baissa, R., Labbassi, K., Launeau, P., Gaudin, A. and Ouajhain, B., Using HySpex SWIR-320m hyperspectral data for the identification and mapping of minerals in hand specimens of carbonate rocks from the Ankloute Formation (Agadir Basin, Western Morocco). *J. Afr. Earth Sci.*, 2011, **61**, 1–9.
36. Clark, R. N., Spectroscopy of rocks and minerals, and principles of spectroscopy, 2011; http://speclab.cr.usgs.gov/PAPERS.refl-mrs/refl4.html

ACKNOWLEDGEMENT. We thank Director, NRSC, Hyderabad and Deputy Director General, Geological Survey of India, Southern Region, for approving this collaborative project and providing necessary technical guidance during the course of the work.

Received 5 December 2011; revised accepted 10 September 2012

Erratum

Indian flying fox in Hamirsir Lake, Bhuj city needs conservation attention

Arun Kumar Roy Mahato, V. Vijay Kumar and Nainesh Patel
[*Curr. Sci.*, 2012, **103**, 354–355]

Caption to Figure 1 is labelled as 'Indian flying fox, *Pteropus giganteus*'. It should read as 'Fulvous fruit bat, *Rousettus leschenaultia*'. We thank Dr N. Singaravelan (yoursings@gmail.com) for bringing the error to our notice.

– Authors